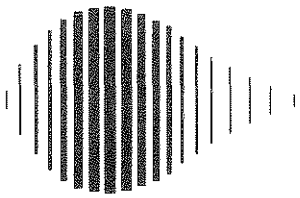

NATIONAL CENTER FOR EARTHQUAKE
ENGINEERING RESEARCH
State University of New York at Buffalo

VERTICAL AND TORSIONAL IMPEDANCES FOR RADIALLY INHOMOGENEOUS VISCOELASTIC SOIL LAYERS

by

K.W. Dotson and A.S. Veletsos
Department of Civil Engineering
Rice University
Houston, TX 77251

Technical Report NCEER-87-0024

December, 1987

This research was conducted at Rice University and was partially supported by the National Science Foundation under Grant No. ECE 86-07591.

NOTICE

This report was prepared by Rice University as a result of research sponsored by the National Center for Earthquake Engineering Research (NCEER). Neither NCEER, associates of NCEER, its sponsors, Rice University, nor any person acting on their behalf:

a. makes any warranty, express or implied, with respect to the use of any information, apparatus, methods, or process disclosed in this report or that such use may not infringe upon privately owned rights; or

b. assumes any liabilities of whatsoever kind with respect to the use of, or for damages resulting from the use of, any information, apparatus, method or process disclosed in this report.

VERTICAL AND TORSIONAL IMPEDANCES FOR RADIALLY INHOMOGENEOUS VISCOELASTIC SOIL LAYERS

by

K.W. Dotson[1] and A.S. Veletsos[2]

December, 1987

Technical Report NCEER-87-0024

NCEER Contract Numbers 86-2034 and 87-1314

NSF Master Contract Number ECE 86-07591

1 Graduate Student, Dept. of Civil Engineering, Rice University
2 Brown and Root Professor, Dept. of Civil Engineering, Rice University

NATIONAL CENTER FOR EARTHQUAKE ENGINEERING RESEARCH
State University of New York at Buffalo
Red Jacket Quadrangle, Buffalo, NY 14261

ACKNOWLEDGMENT

This study was supported in part by an ARCS Foundation Scholarship awarded through Rice University to K. W. Dotson, and in part by Grants 86-2034 and 87-1314 from the National Center for Earthquake Engineering Research, State University of New York at Buffalo. This support is appreciated greatly.

ABSTRACT

A study of the dynamic impedances of thin, infinite viscoelastic soil layers with a circular hole is made considering a continuous, ramp-like radial variation for the shear modulus of the material. Both vertically and torsionally excited systems are examined. The impedances are evaluated over wide ranges of the parameters involved and compared with those obtained both for homogeneous layers, and for inhomogeneous layers with discontinuous variations in shear modulus. In addition, a simple approximate method of analysis based on the Galerkin approach is presented for vertically excited layers, and it is used to assess the parameters that control their high-frequency response.

TABLE OF CONTENTS

LIST OF ILLUSTRATIONS

SECTION 1
INTRODUCTION

Whereas the dynamic impedances of thin homogeneous soil layers are well established and have been used extensively in studies of piles and other embedded foundations (e.g., references 3,4,5), those for inhomogeneous layers have received comparatively little attention.

The earliest study of inhomogeneous layers appears to have been made by Novak and Sheta [6], who, in an effort to provide for the effects of the typically reduced resistance of soils in the immediate vicinity of the foundation, proposed the use of a composite viscoelastic layer with a weakened annular boundary zone around the foundation. In the original analysis of this problem, the shear modulus of the layer for each zone was considered to be constant, and the mass of the boundary zone was presumed to be negligible.

Subsequent analyses [7,8,9] revealed that, even when the boundary zone is fairly narrow, its inertia effects may be substantial and should not, in general, be neglected. These analyses have further revealed that the variations with frequency of the layer impedances may be highly undulatory for abrupt variations in shear modulus. A consequence of the wave reflections from the discontinuous interface of the two zones, these undulations would not be expected to occur for layers with more realistic, continuous property variations.

The primary purpose of this paper is to evaluate the dynamic impedances for viscoelastic layers with continuous, ramp-like variations in shear modulus, and to compare the results with those obtained for homogeneous layers as well as for composite layers with discontinuous modulus variations. Only vertically and torsionally excited layers are examined. A companion study of horizontally excited layers has been reported recently in reference 9.

The shear modulus for the boundary zone of the layer in the study reported herein is assumed to increase exponentially in the radial direction, and

all other material properties are considered to be constant within each zone. In addition to being more nearly representative of actual conditions, the particular variation considered leads to simple, closed-form solutions for the governing equations of motion.

A secondary objective of this paper is to present a relatively simple method of analysis for the system based on the Galerkin approach, and to demonstrate the utility and range of applicability of this approach.

The impedances of soil layers with linearly increasing radial variation of shear modulus within the boundary zone have also been examined by Lakshmanan and Minai [2]. Although the inertia effects of the boundary zone were duly considered in this study, the width of the boundary zone and the relative values of the shear moduli for the two zones could not be varied independently by the method of analysis employed.

SECTION 2
SYSTEM CONSIDERED

The system examined is similar to that employed in reference 8. It is a viscoelastic layer of unit depth and infinite extent with a circular hole of radius R, as shown in figure 2-1. The layer consists of two concentric zones: a narrow annular boundary zone of disturbed material and width ΔR, and a semi-infinite outer zone of undisturbed material. The radius of the interface of the two zones is denoted by R_o. Unlike the layer examined in reference 8, however, for which the material properties of the inner zone were considered to be constant, in the present study, the complex-valued shear modulus of the layer, $G^*(\xi)$, is considered to increase exponentially according to the expressions

$$G^*(\xi) = \begin{cases} G_i(1 + i\tan\delta_i)\,\xi^m & \text{for } 1 \leq \xi \leq \xi_o \quad (1a) \\ G_o(1 + i\tan\delta_o) & \text{for } \xi \geq \xi_o \quad (1b) \end{cases}$$

in which $\xi = r/R$; $\xi_o = R_o/R$; r = the radial distance to an arbitrary point; $i = \sqrt{-1}$; m = a positive constant; G_i and G_o are the shear moduli for the innermost boundary and outer zone, respectively; and $\tan\delta_i$ and $\tan\delta_o$ are constants representing the material damping factors for the two zones. At $\xi = \xi_o$, the real parts of equations (1a) and (1b) are considered to be equal. Accordingly,

$$G_i\xi_o^m = G_o \quad (2)$$

and unless $\tan\delta_i = \tan\delta_o$, the complex-valued shear modulus is discontinuous at $\xi = \xi_o$. It is important to note that, for a specified value of m, the ratio G_o/G_i and the relative width of the boundary zone, $\Delta R/R$, cannot be varied arbitrarily. Indeed, on noting that $\xi_o = (R + \Delta R)/R$, one obtains the following relationship between $\Delta R/R$ and G_o/G_i from equation (2):

$$\frac{\Delta R}{R} = \left(\frac{G_o}{G_i}\right)^{1/m} - 1 \quad (3)$$

The real part of $G^*(\xi)$ will be denoted by $G(\xi)$.

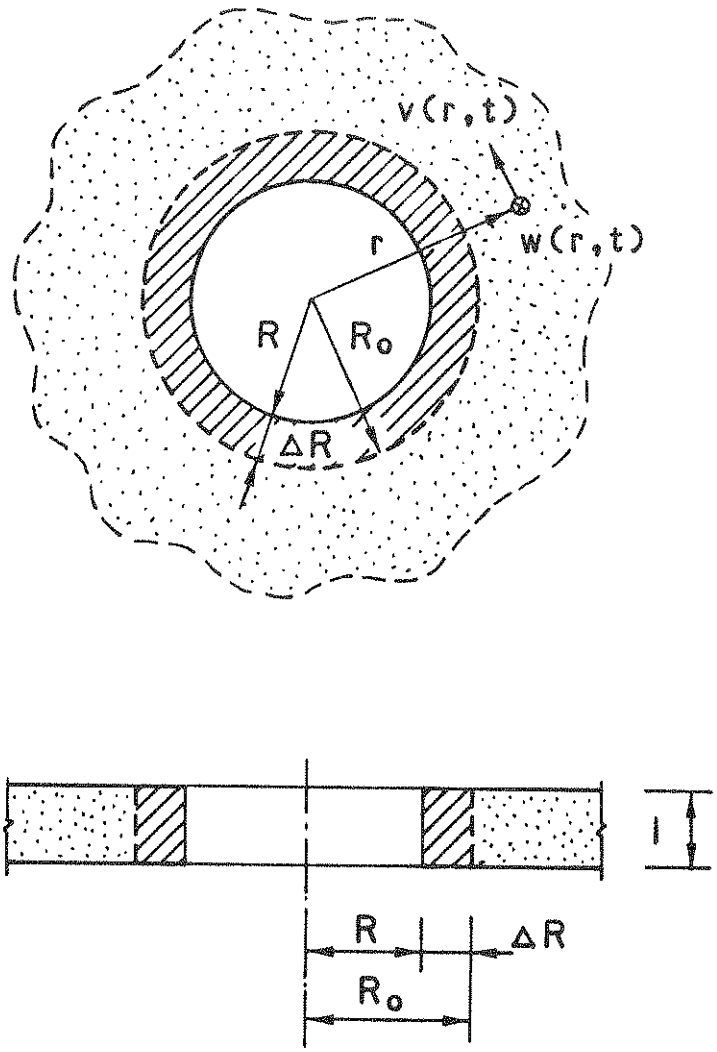

Figure 2-1. Composite Layer Considered

For each mode of vibration, the layer is presumed to deform in pure shear, and only small amplitude oscillations are considered. It is desired to evaluate the dynamic impedances of the layer, K_w and K_θ, defined as the complex-valued amplitudes of the vertical force and torque which are necessary to induce, respectively, a vertical displacement and a rotation of unit amplitude along the boundary of the central hole.

In reference 2, the radial variation of the shear modulus within the boundary zone was considered to be linear, m = 1, and the layer impedances were evaluated only for the combinations of $\Delta R/R$ and G_o/G_i defined by equation (3). By letting m be arbitrary in the present study, the ratios $\Delta R/R$ and G_o/G_i may, in effect, be varied arbitrarily.

In figure 2-2 are shown the variations in shear modulus obtained for several different combinations of $\Delta R/R$ and G_o/G_i, along with the associated values of m. Note that these variations are not materially different from the linear variation considered in the companion study of horizontally excited layers [9], and are, in fact, more realistic than the linear in that severe disturbances, represented by the higher values of G_o/G_i, are felt over greater distances than are moderate disturbances.

The subscript i will be used to identify material properties for the innermost boundary and the subscript o will identify the corresponding properties for the outer zone. For the solutions presented herein, the mass density of the layer, ρ, is considered to be the same throughout.

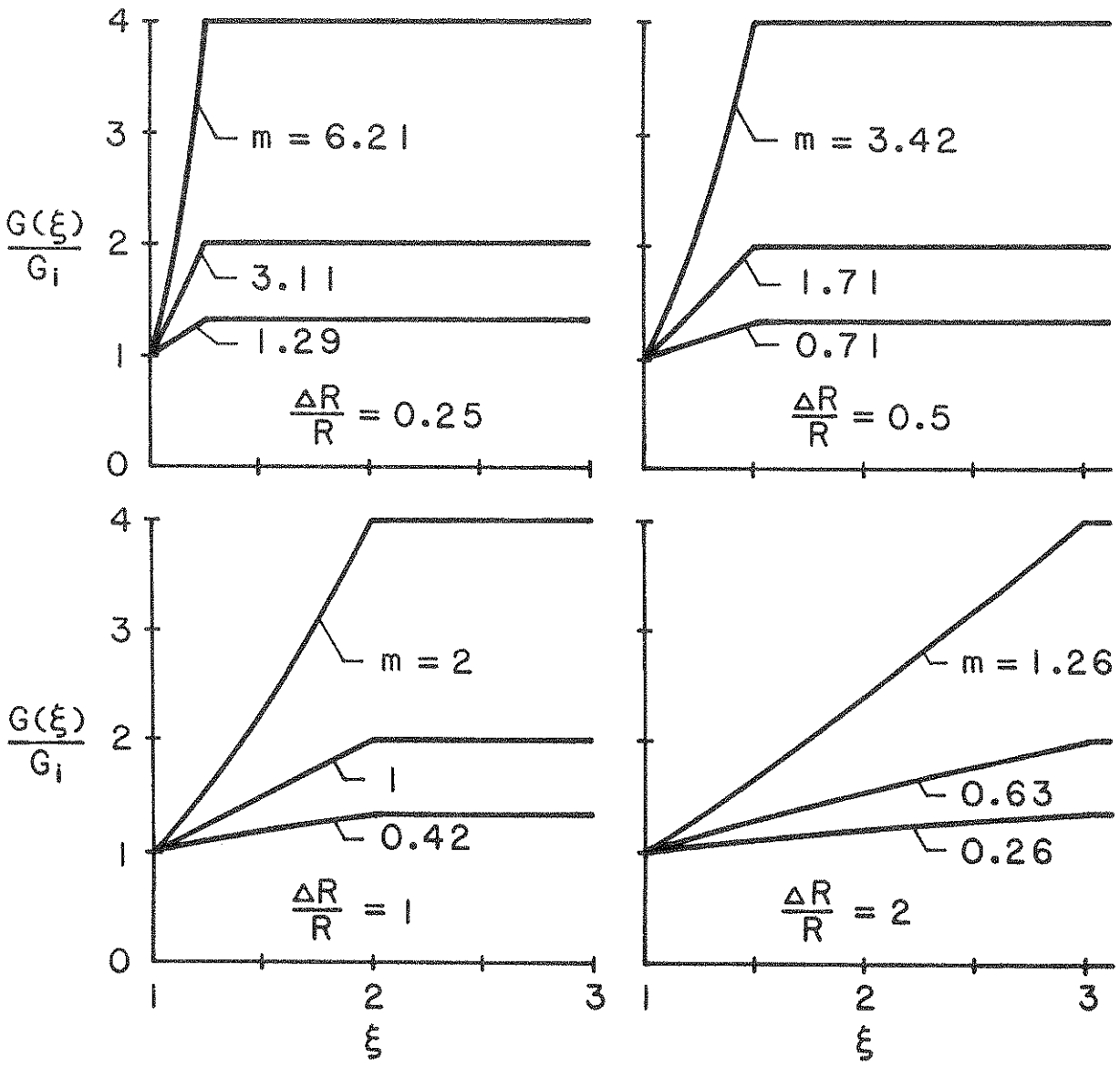

Figure 2-2. Ramp-Like Variations of Shear Modulus Considered

SECTION 3
ANALYSIS OF SYSTEM

Let $w(\xi,t)$ be the vertical displacement at an arbitrary point and time t induced by the vertical excitation, and $v(\xi,t)$ be the corresponding circumferential displacement induced by the torsional excitation. These displacements are of the form,

$$w(\xi,t) = w e^{i\omega t} \tag{4a}$$

$$\text{and} \quad v(\xi,t) = v e^{i\omega t} \tag{4b}$$

in which ω = the circular frequency of the excitation and of the resulting steady-state response, and w and v are complex-valued displacement amplitudes that are functions of the dimensionless position coordinate, ξ.

3.1 Vertically Excited Layer

The differential equations for the displacement amplitudes of the vertically excited layer, deduced from expressions given in reference 8, are

$$\xi^2 \frac{d^2w}{d\xi^2} + (m+1)\xi \frac{dw}{d\xi} - \lambda_i^2 \xi^{2-m} w = 0 \qquad \text{for } 1 \leq \xi \leq \xi_o \tag{5a}$$

$$\xi^2 \frac{d^2w}{d\xi^2} + \xi \frac{dw}{d\xi} - \lambda_o^2 \xi^2 w = 0 \qquad \text{for } \xi \geq \xi_o \tag{5b}$$

in which

$$\lambda_i = \frac{ia_i}{\sqrt{1 + i\tan\delta_i}} \tag{6}$$

$$a_i = \frac{\omega R}{v_{si}} \tag{7}$$

$v_{si} = \sqrt{G_i/\rho}$ = the velocity of shear wave propagation in a medium with the properties of the soil at the boundary of the hole;

$$\lambda_o = \frac{ia_o}{\sqrt{1 + i\tan\delta_o}} \tag{8}$$

$$a_o = \frac{\omega R}{v_{so}} \tag{9}$$

and $v_{so} = \sqrt{G_o/\rho}$ = the velocity of shear wave propagation in a medium with the properties of the outer zone.

The solutions of these equations are

$$w = \xi^{-m/2}\,[A_w K_{\kappa-1}(\kappa\lambda_i\xi^{1/\kappa}) + B_w I_{\kappa-1}(\kappa\lambda_i\xi^{1/\kappa})] \quad \text{for } 1 \leq \xi \leq \xi_o \tag{10a}$$

$$\text{and} \quad w = C_w K_o(\lambda_o\xi) + D_w I_o(\lambda_o\xi) \quad \text{for } \xi \geq \xi_o \tag{10b}$$

in which $\kappa = 2/(2 - m)$; I_κ and K_κ are modified Bessel functions of order κ of the first and second kind, respectively; and A_w, B_w, C_w and D_w are complex-valued constants of integration which are determined by requiring that the displacement amplitude be unity at the boundary of the hole, that the displacements vanish as $\xi \to \infty$, and that the displacements and stresses be continuous at the interface of the two zones.

Satisfaction of these boundary conditions leads to $D_w = 0$ and to the following systems of algebraic equations for the determination of the remaining constants:

$$\begin{bmatrix} K_{\kappa-1}(\kappa\lambda_i) & I_{\kappa-1}(\kappa\lambda_i) & 0 \\ K_{\kappa-1}(\kappa\lambda_i\xi_o^{1/\kappa}) & I_{\kappa-1}(\kappa\lambda_i\xi_o^{1/\kappa}) & -\xi_o^{m/2} K_o(\lambda_o\xi_o) \\ -K_\kappa(\kappa\lambda_i\xi_o^{1/\kappa}) & I_\kappa(\kappa\lambda_i\xi_o^{1/\kappa}) & \chi K_1(\lambda_o\xi_o) \end{bmatrix} \begin{Bmatrix} A_w \\ B_w \\ C_w \end{Bmatrix} = \begin{Bmatrix} 1 \\ 0 \\ 0 \end{Bmatrix} \tag{11}$$

in which $\chi = \sqrt{G_o^*/G_i^*}$. With the integration constants evaluated, the impedance of the vertically excited layer, K_w, is computed from

$$K_w = -2\pi G_i^* \frac{dw}{d\xi}\Big|_{\xi=1} \tag{12a}$$

$$\text{or } K_w = 2\pi G_i^* \lambda_i [A_w K_\kappa(\kappa\lambda_i) - B_w I_\kappa(\kappa\lambda_i)] \tag{12b}$$

3.2 Torsionally Excited Layer

The differential equations governing the amplitude of the circumferential displacement of such a layer are:

$$\xi^2 \frac{d^2v}{d\xi^2} + (m+1)\xi \frac{dv}{d\xi} - (\lambda_i^2 \xi^{2-m} + m + 1)\, v = 0 \quad \text{for } 1 \leq \xi \leq \xi_o \tag{13a}$$

$$\xi^2 \frac{d^2v}{d\xi^2} + \xi \frac{dv}{d\xi} - (\lambda_o^2 \xi^2 + 1)v = 0 \quad \text{for } \xi \geq \xi_o \tag{13b}$$

and their solutions are

$$v = \xi^{-m/2} [A_\theta K_{2\kappa-1}(\kappa\lambda_i \xi^{1/\kappa}) + B_\theta I_{2\kappa-1}(\kappa\lambda_i \xi^{1/\kappa})] \quad \text{for } 1 \leq \xi \leq \xi_o \tag{14a}$$

$$\text{and } v = C_\theta K_1(\lambda_o \xi) + D_\theta I_1(\lambda_o \xi) \quad \text{for } \xi \geq \xi_o \tag{14b}$$

in which $D_\theta = 0$, and A_θ, B_θ and C_θ are complex-valued constants of integration determined from the solution of the following system of algebraic equations:

$$\begin{bmatrix} K_{2\kappa-1}(\kappa\lambda_i) & I_{2\kappa-1}(\kappa\lambda_i) & 0 \\ K_{2\kappa-1}(\kappa\lambda_i \xi_o^{1/\kappa}) & I_{2\kappa-1}(\kappa\lambda_i \xi_o^{1/\kappa}) & -\xi_o^{m/2} K_1(\lambda_o \xi_o) \\ -K_{2\kappa}(\kappa\lambda_i \xi_o^{1/\kappa}) & I_{2\kappa}(\kappa\lambda_i \xi_o^{1/\kappa}) & \chi K_2(\lambda_o \xi_o) \end{bmatrix} \begin{Bmatrix} A_\theta \\ B_\theta \\ C_\theta \end{Bmatrix} = \begin{Bmatrix} R \\ 0 \\ 0 \end{Bmatrix} \tag{15}$$

The rotational impedance, K_θ, is then determined from

$$K_\theta = -2\pi G_i^* R \left(\frac{dv}{d\xi} - \frac{v}{\xi}\right)\Big|_{\xi=1} \tag{16a}$$

$$\text{or } K_\theta = 2\pi G_i^* R \lambda_i \left[A_\theta K_{2\kappa}(\kappa\lambda_i) - B_\theta I_{2\kappa}(\kappa\lambda_i)\right] \tag{16b}$$

3.3 A Special Case

For the special case of $m = 2$, the quantity ξ disappears from the rightmost terms of the left hand side of equations (5a) and (13a), and the solutions presented so far are not applicable. The correct expressions for the displacement amplitudes in this case are given in the Appendix.

SECTION 4
PRESENTATION AND ANALYSIS OF RESULTS

4.1 Format of Presentation

It is desirable to express equations (12) and (16) in the form employed in reference 8 as

$$K_w = \pi G_i(\alpha_w + ia_i\beta_w) \tag{17}$$

$$\text{and} \quad K_\theta = 3\pi G_i R^2(\alpha_\theta + ia_i\beta_\theta) \tag{18}$$

in which α_w, α_θ, β_w and β_θ are dimensionless coefficients that depend on a_i, $\Delta R/R$, G_o/G_i, $\tan\delta_i$ and $\tan\delta_o$. The real part in each of these expressions represents the force component that is in phase with the motion, and the imaginary part represents the component that is 90° out of phase.

In equivalent, spring-dashpot representations of the soil layer, the spring stiffnesses are represented by the real parts of equations (17) and (18), and the damping coefficients, c_w and c_θ, are related to β_w and β_θ by the expressions

$$c_w = \pi\beta_w \frac{G_i R}{v_{si}} \tag{19}$$

$$\text{and} \quad c_\theta = 3\pi\beta_\theta \frac{G_i R^3}{v_{si}} \tag{20}$$

Note that unlike the format employed by Novak and Sheta [6], in which K_w and K_θ were expressed in terms of the shear modulus of the outer zone, equations (17) and (18) are expressed in terms of the shear modulus along the boundary of the hole. Note further that the frequency parameter a_i has been added in front of the factors β_w and β_θ. When expressed in this form, the high frequency limits of α_w and α_θ for a homogeneous layer without material damping are unity, and the corresponding values of β_w and β_θ are 2 and 2/3, respectively.

4.2 Results

The results obtained for vertically excited layers with no material damping ($\tan\delta_i = \tan\delta_o = 0$) are shown in figure 4-1 for several different combinations of $\Delta R/R$ and G_o/G_i, and the corresponding data for torsionally excited layers are shown in figure 4-2. The values of m for the combinations of $\Delta R/R$ and G_o/G_i considered are identified in figure 2-2.

The general trends of the curves in figures 4-1 and 4-2 and of the corresponding curves presented in reference 8 for layers with abrupt variations in shear modulus are similar, except for the following:

1. The present curves are not nearly as undulatory as those reported previously. Considering that the variation of the shear modulus for the present solutions is continuous, this result is not surprising. What might be surprising is that the curves are undulatory at all. Contributed by the discontinuity in the slope of the G-diagram at the interface of the two zones, the amplitudes of these oscillations are effectively proportional to the magnitude of the slope discontinuity, increasing with increasing G_o/G_i and decreasing $\Delta R/R$. However, these undulations are generally of small amplitude and, as demonstrated in a later section, they are further suppressed for layers with finite values of material damping.

2. The abscissas of the curves in figures 4-1 and 4-2 are essentially stretched-out versions of those for the corresponding curves with discontinuous variations in G presented in reference 8. For example, whereas the peak of the α_w curve for $\Delta R/R = 0.5$ and $G_o/G_i = 4$ in figure 4-1 occurs at $a_i \simeq 3.3$, the peak of the corresponding curve in reference 8 occurs at $a_i \simeq 1.3$. Similarly, whereas the point of intersection of the β_w curves in figure 4-1(b) occurs at $a_i \simeq 2.8$, the corresponding point for the curves in reference 8 occurs at $a_i \simeq 0.8$.

The latter trends are consequences of the fact that the inner zone of the layer for the continuous variation in shear modulus is stiffer, and hence has a higher effective shear wave velocity, than for the discontinuous variation. It follows that a prescribed value of a_i for the continuous

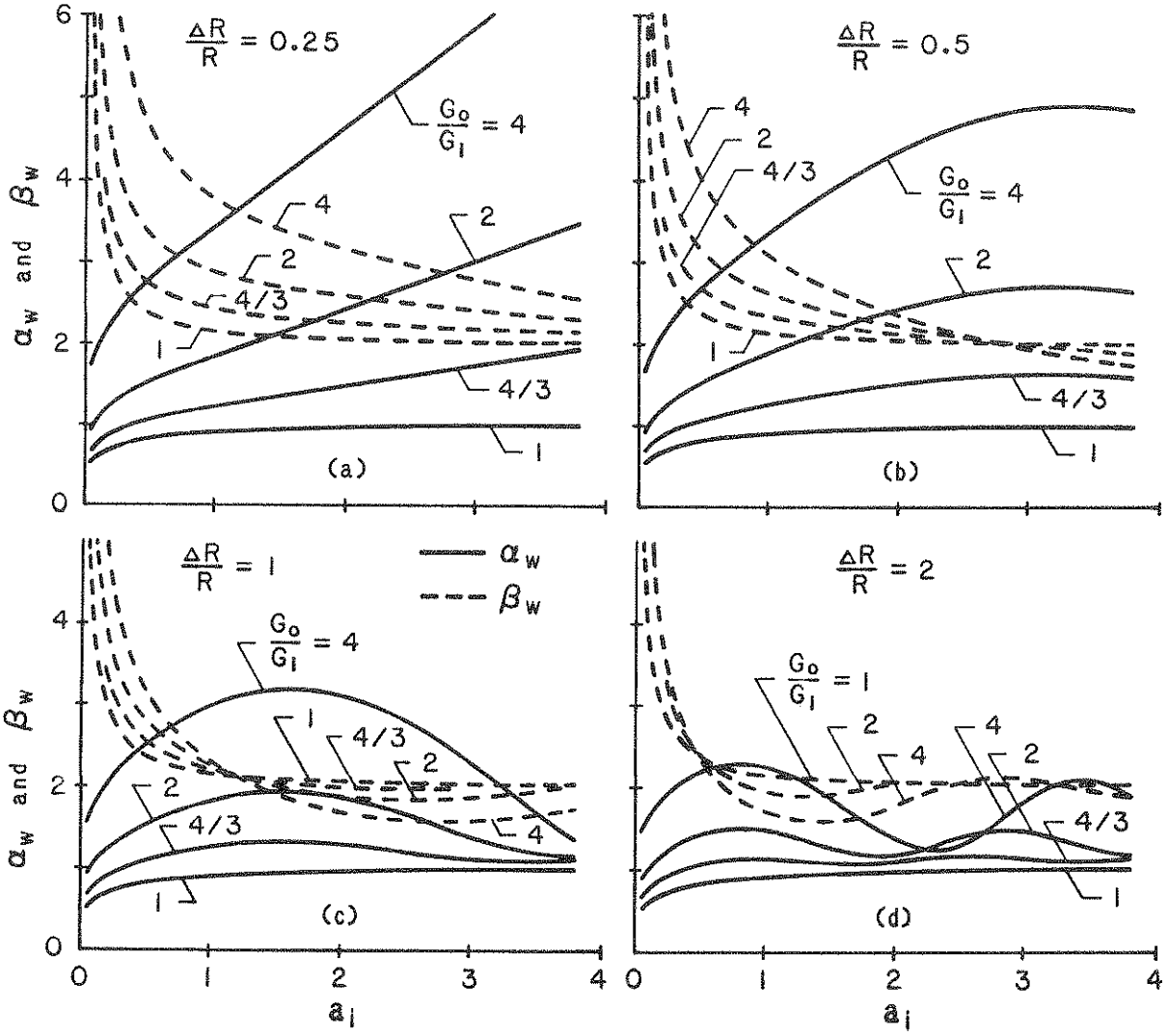

Figure 4-1. Impedance Coefficients for Vertically Excited Layers; $\tan \delta_i = \tan \delta_o = 0$

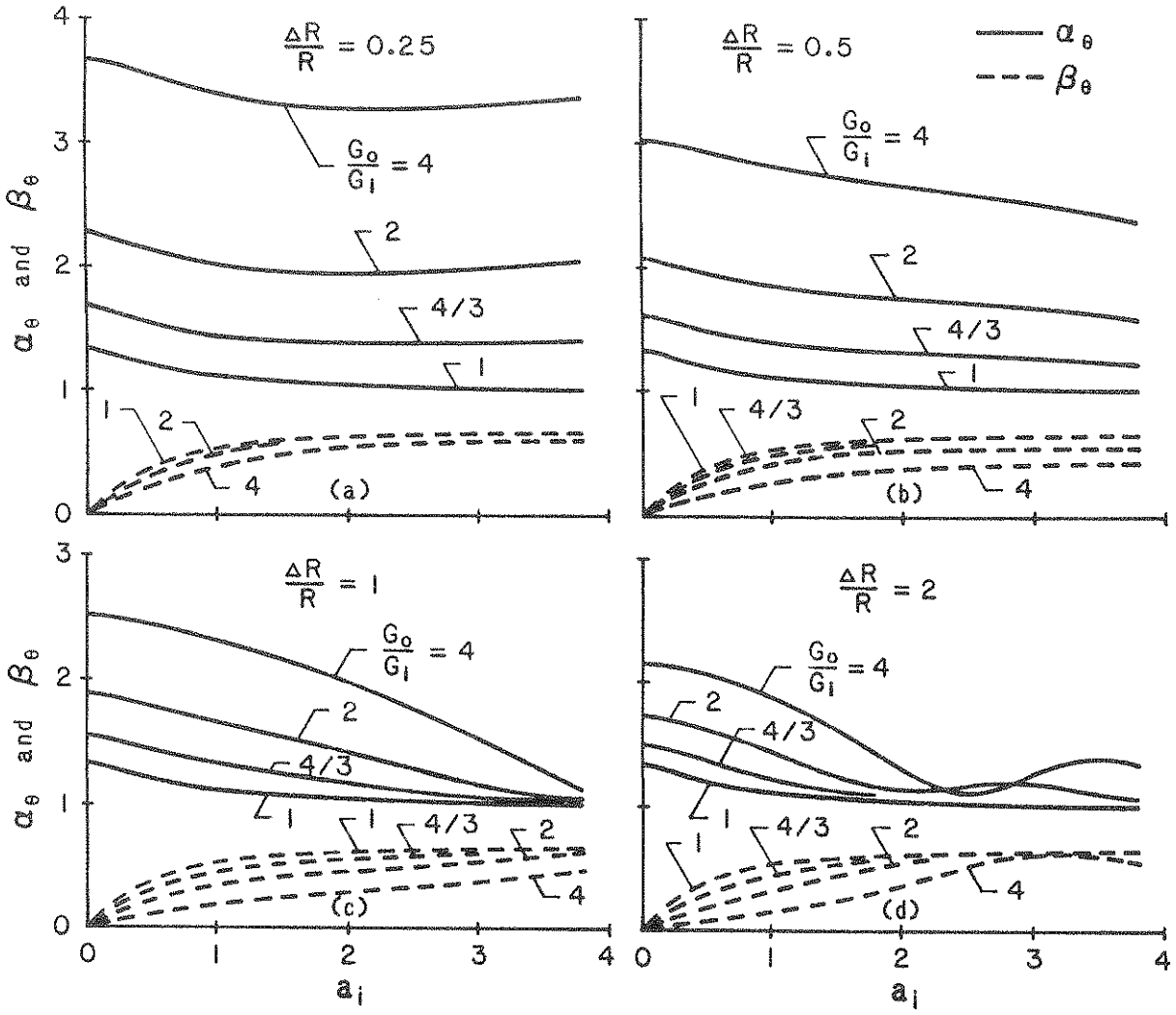

Figure 4-2. Impedance Coefficients for Torsionally Excited Layers; $\tan \delta_i = \tan \delta_o = 0$

variation corresponds to a reduced value for the discontinuous variation; and the larger the value of G_o/G_i, the larger is the reduction.

4.3 Comparison for Constant Areas

As a further indication of the interrelationship of the impedance functions for the ramp variation of shear modulus examined herein and the discontinuous variation considered in reference 8, a comparison is made in figure 4-3 of the results obtained for layers with no material damping and $G_o/G_i = 2$. The widths of the boundary zones in these solutions are taken such that the areas under the $G(\xi)$-diagrams for the two cases are equal.

For the layer with abruptly varying shear modulus, two different widths are considered for the boundary zone: A very narrow zone with a value of $\Delta R/R = 0.1$; and a fairly wide zone with a value of $\Delta R/R = 1$. The corresponding values of $\Delta R/R$ and m for the exponentially increasing variation are 0.18 and 4.10 for the narrow zone, and 2.16 and 0.60 for the wide zone.

The results for the thin boundary zone are displayed in the upper part of figure 4-3 and those for the wide boundary zone are displayed in the lower part. The excellent agreement of the results in the first case indicates that the response of the system for very narrow boundary zones is effectively controlled by the area under the $G(\xi)$ diagram. By contrast, for the wide boundary zones, the response is affected significantly by the detailed characteristics of the $G(\xi)$ diagram, particularly by the nature of its discontinuities. The consequences of wave reflections due to a discontinuity in the slope of $G(\xi)$ are clearly not as important as those due to a discontinuity in $G(\xi)$ itself. The difference is particularly large for vertically excited layers.

4.4 Static Values of Impedances

The vertically excited layer offers no resistance to static loads, with the result that α_w in figure 4-1 tends to zero as $a_i \to 0$. By contrast, the torsionally excited layer is statically stable, and the curves for α_θ in figure 4-2 approach non-zero values.

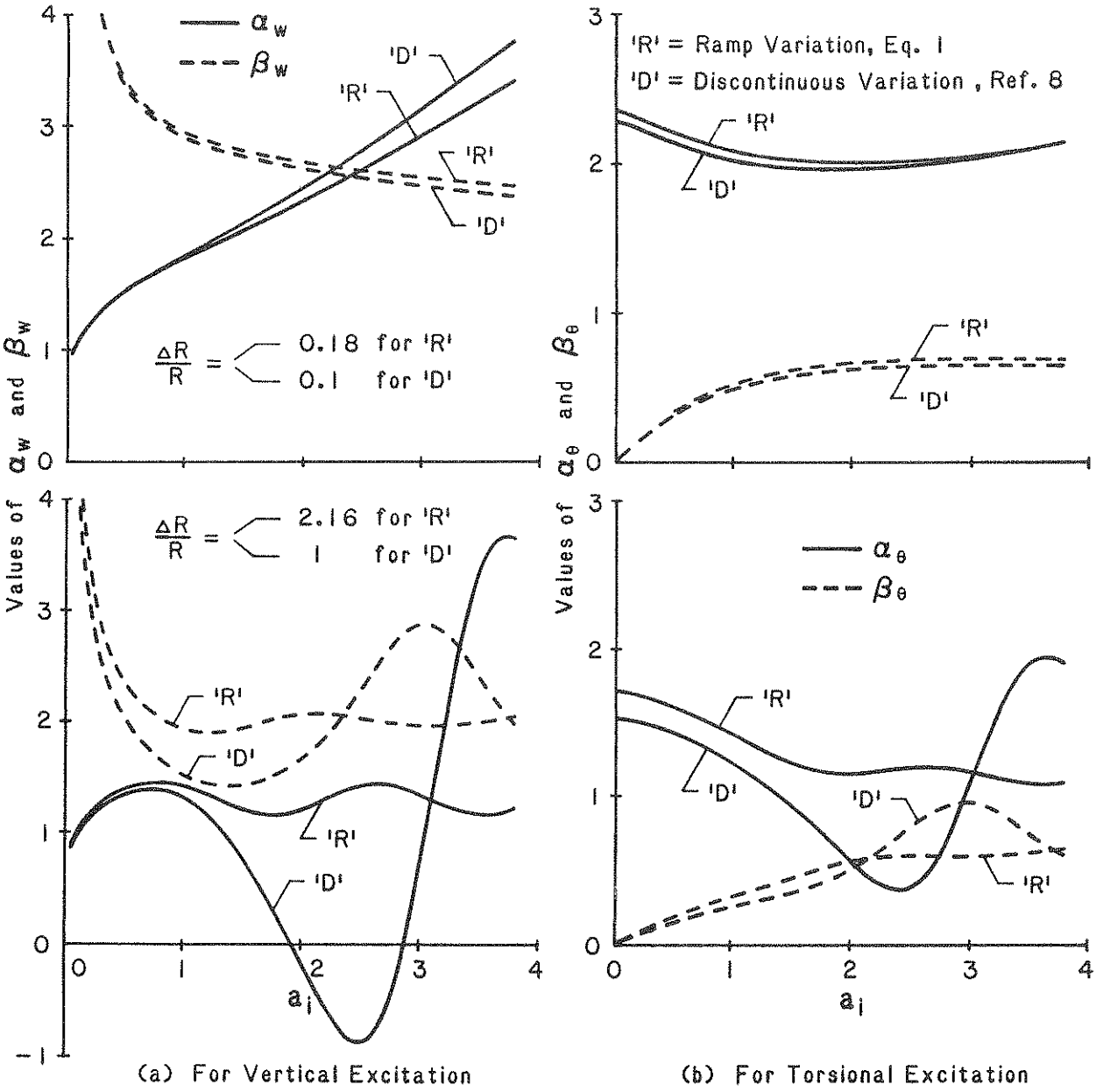

Figure 4-3. Comparisons of Impedance Coefficients for Soil Layers with Ramp and Discontinuous Variations in Shear Modulus; $G_o/G_i = 2$, $\tan \delta_i = \tan \delta_o = 0$

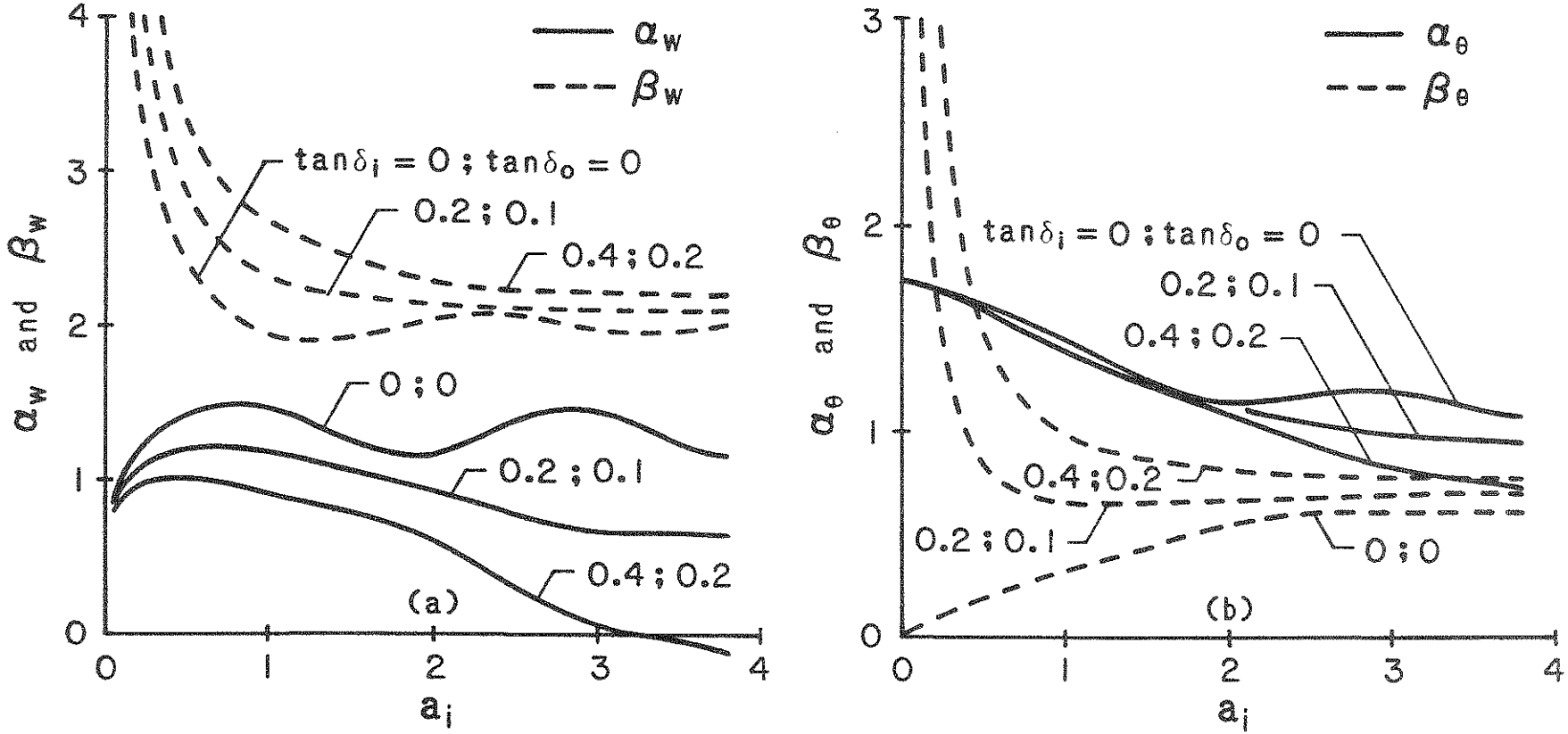

Figure 4-4. Effects of Soil Material Damping on Layer Impedances; $G_o/G_i = 2$, $\Delta R/R = 2$, $m = 0.63$

The "static" impedance of a torsionally excited viscoelastic layer may be deduced from equations (13) by taking $\lambda_i = \lambda_o = 0$. The solutions of the resulting equations are

$$v = A_\theta \xi^{-(m+1)} + B_\theta \xi \qquad \text{for } 1 \leq \xi \leq \xi_o \tag{21a}$$

$$\text{and } v = C_\theta \xi^{-1} + D_\theta \xi \qquad \text{for } \xi \geq \xi_o \tag{21b}$$

from which, on satisfying the appropriate boundary and interface conditions, one obtains

$$(K_\theta)_{a_i=0} = 4\pi G_i^* R^2 \frac{1 + \frac{m}{2}}{1 + \left(\frac{G_i}{G_o}\right)^{(2+m)/m} \left[(1 + \frac{m}{2}) \frac{1 + i\tan\delta_i}{1 + i\tan\delta_o} - 1\right]} \tag{22}$$

4.5 Effects of Material Damping

The impedance functions for elastic layers with $G_o/G_i = 2$ and $\Delta R/R = 2$ presented in figures 4-1(d) and 4-2(d) are compared in figure 4-4 with the corresponding functions obtained for a viscoelastic layer with $\tan\delta_i = 2\tan\delta_o$. As would be expected from available information about homogeneous layers [4] and composite layers with abrupt variations in shear modulus [8], material damping increases the damping capacity of the layer, decreases its stiffness, and suppresses the undulations in the plots for both of these quantities. The increase in damping is particularly large for the torsional mode of vibration, especially at the low values of the frequency parameter, for which the effects of radiation damping are small.

SECTION 5
LAYERS WITH SMOOTH VARIATIONS IN SHEAR MODULUS

The impedances of vertically excited layers are evaluated in this section for radial variations in shear modulus that are continuous both in the function itself and its derivatives. The analysis is implemented approximately by the Galerkin approach using a single approximating function. Special emphasis is paid to the behavior of the system at high frequencies.

The complex-valued shear modulus is taken in the form

$$G^*(\xi) = G_i g(\xi) \tag{23}$$

in which $g = g(\xi)$ = a complex-valued dimensionless function of ξ, defined by

$$g(\xi) = \frac{G_o}{G_i} - \left(\frac{G_o}{G_i} - 1\right) e^{-n(\xi-1)} + i \tan \delta_i \tag{24}$$

and n is a positive constant. The real part of this expression defines the variation of the shear modulus, whereas the ratio of the imaginary and real parts defines the material damping of the system. Note that whereas the shear modulus increases monotonically with increasing ξ, the damping factor exhibits the opposite trend. In particular, as $\xi \to \infty$, G tends to G_o, and the material damping factor tends to

$$\tan \delta_o = (G_i/G_o) \tan \delta_i \tag{25}$$

The variations of these quantities with ξ are displayed in figure 5-1 for four different values of n.

5.1 Analysis of Layer

The differential equation for the displacement amplitude, w, is

$$\xi^2 g \frac{d^2w}{d\xi^2} + \left(\xi^2 \frac{dg}{d\xi} + \xi g\right) \frac{dw}{d\xi} + a_i^2 \xi^2 w = 0 \tag{26}$$

This equation is obtained from the equilibrium of vertical forces,

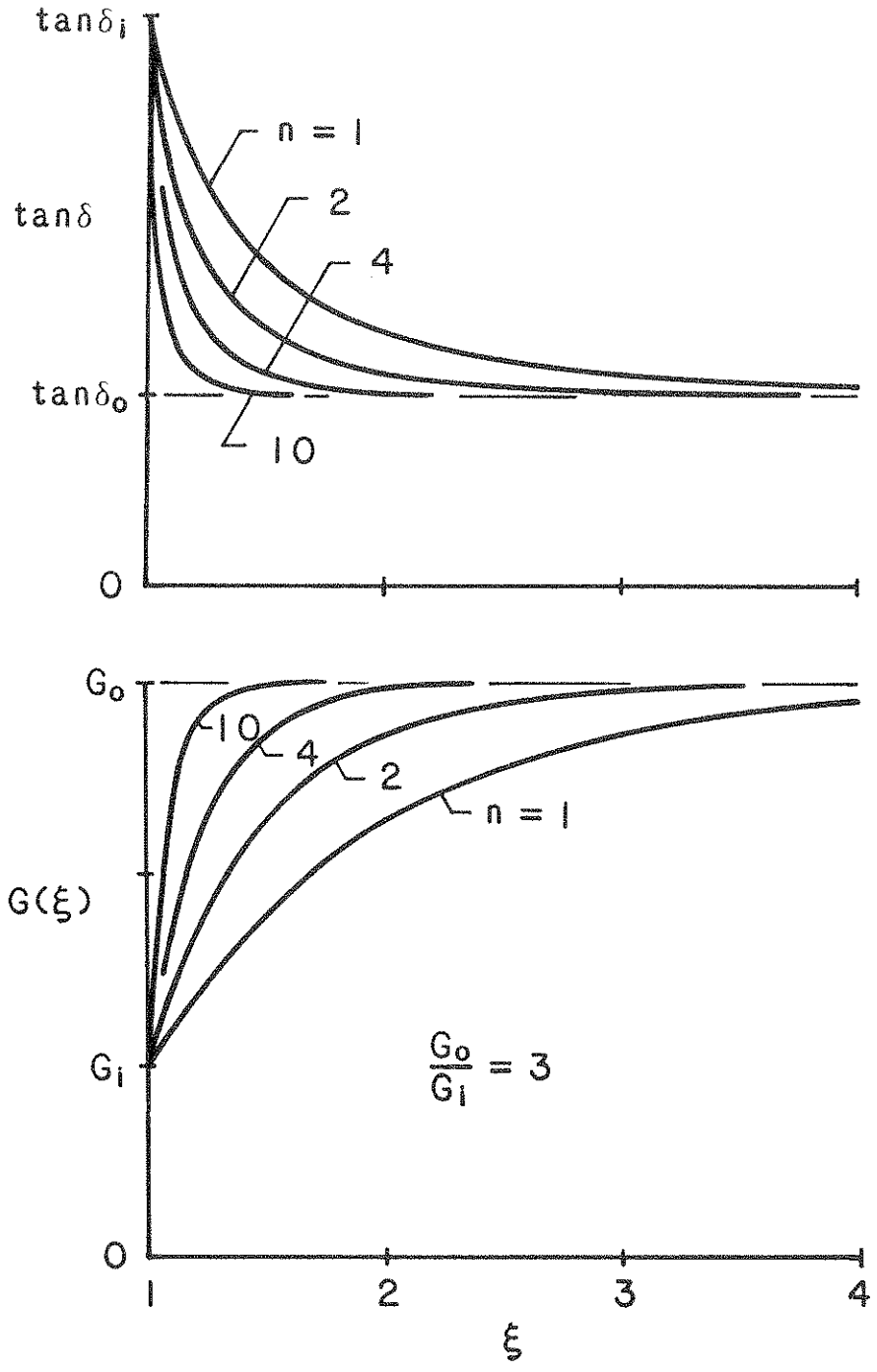

Figure 5-1. Radial Variations of Material Properties Defined by Equation (23)

$$\tau_{rz} + r\frac{d\tau_{rz}}{dr} = -\rho r \omega^2 w \tag{27}$$

in which the shearing stress, τ_{rz}, is related to w by

$$\tau_{rz} = G^* \frac{dw}{dr} \tag{28}$$

and G^* is given by the right-hand member of equation (23).

The solution of equation (26) is taken approximately in the form

$$w = \phi = e^{-\gamma(\xi-1)} \tag{29}$$

in which γ is a complex-valued dimensionless parameter. Equation (29) satisfies the condition of unit displacement amplitude at the boundary of the central hole. In order that it also represent waves that propagate away from the hole with amplitudes that decay with increasing ξ, both the real and imaginary parts of γ must be positive, i.e.,

$$\mathrm{Re}(\gamma) > 0 \tag{30a}$$

$$\mathrm{Im}(\gamma) > 0 \tag{30b}$$

On substituting the approximating function ϕ into equation (26) and requiring that the integral over the range $1 \leq \xi \leq \infty$ of the product of the approximating function and the residual or error function vanish, one obtains

$$\int_1^\infty [\xi^2 g \phi \frac{d^2\phi}{d\xi^2} + (\xi^2 \frac{dg}{d\xi} + \xi g)\phi \frac{d\phi}{d\xi} + a_i^2 \xi^2 \phi^2] d\xi = 0 \tag{31}$$

Evaluation of this integral leads to the seventh order polynomial

$$\sum_{j=0}^{7} C_j \gamma^j = 0 \tag{32}$$

in which

$$C_o = \frac{1}{4} a_i^2 n^3 \tag{33a}$$

$$C_1 = \frac{1}{2} a_i^2 (n^3 + 3n^2) \tag{33b}$$

$$C_2 = \frac{1}{2}a_i^2(n^3 + 6n^2 + 6n) \tag{33c}$$

$$C_3 = a_i^2(3n^2 + 6n + 2) \tag{33d}$$

$$C_4 = a_i^2(6n + 4) + \frac{1}{2}\frac{G_o^*}{G_i}n^3 - (\frac{G_o}{G_i} - 1)(n^3 + n^2 + n) \tag{33e}$$

$$C_5 = 4a_i^2 + 3\frac{G_o^*}{G_i}n^2 - (\frac{G_o}{G_i} - 1)(5n^2 + 2n) \tag{33f}$$

$$C_6 = 6\frac{G_o^*}{G_i}n - 8(\frac{G_o}{G_i} - 1)n \tag{33g}$$

$$C_7 = 4\frac{G_o^*}{G_i} - 4(\frac{G_o}{G_i} - 1) = 4(1 + i\tan\delta_i) \tag{33h}$$

Of the seven values of γ which satisfy equation (32), only one has been found also to satisfy equations (30). On making use of this particular value of γ, the impedance of the layer is determined from

$$K_w = -2\pi G_i^* \frac{d\phi}{d\xi}\Big|_{\xi=1} = 2\pi G_i^* \gamma \tag{34}$$

5.2 Reliability of Solution

A measure of the reliability of the approximate procedure is provided in figure 5-2, in which the impedance coefficients for a homogeneous layer obtained by this approach are compared with the corresponding exact values for $\tan\delta = 0$ and 0.20. Equation (32) in this case reduces to

$$(1 + i\tan\delta_o)\gamma^4 + a_o^2\gamma^2 + a_o^2\gamma + \frac{1}{2}a_o^2 = 0 \tag{35}$$

It is observed that whereas the agreement between the two sets of data is excellent at the larger values of a_o, it deteriorates at the smaller values, resulting in errors that may exceed 20% for $a_o < 0.4$. However, the errors in the individual coefficients are of opposite signs, and the maximum error in the amplitude of the impedance (represented by the square root of the sum of the squares of α_w and β_w) is generally quite small.

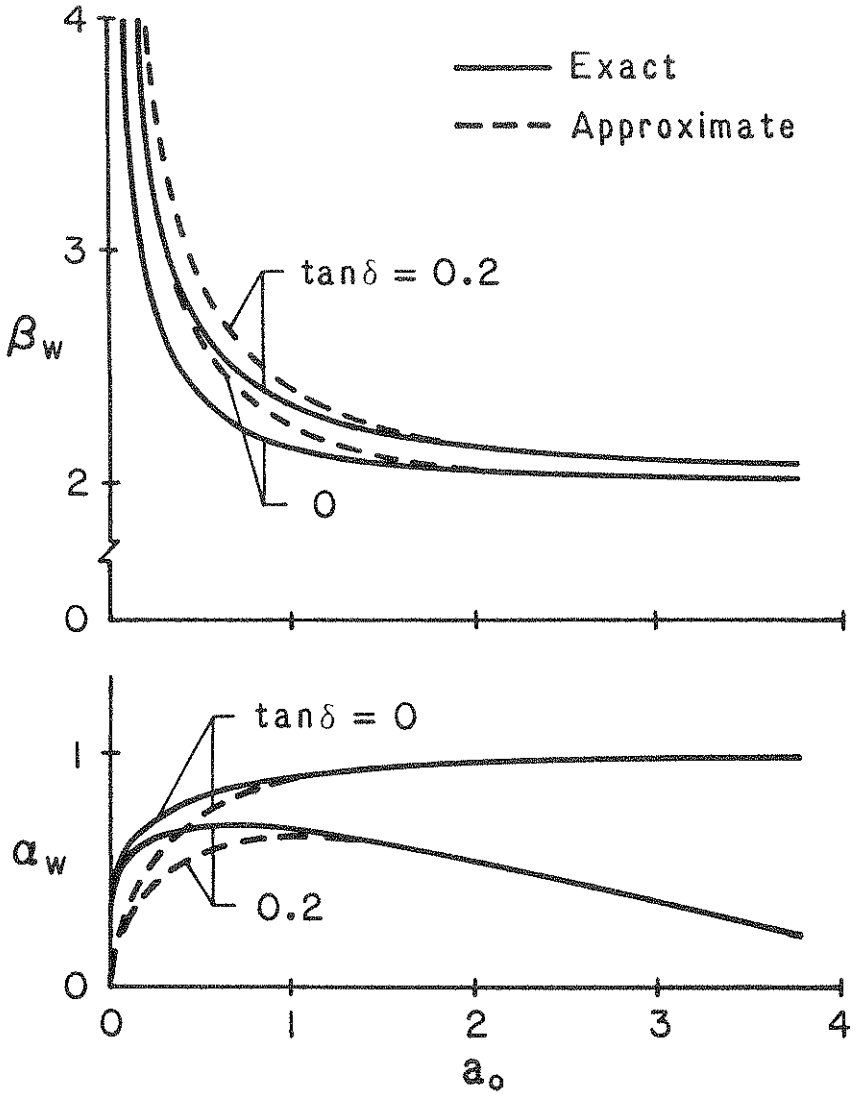

Figure 5-2. Comparisons of Exact and Approximate Impedance Coefficients for Vertically Excited Homogeneous Layer

5.3 Presentation of Results

The impedance coefficients for layers with the variation of shear modulus defined by equations (23) and (24) is given in figure 5-3 for several different combinations of G_o/G_i and n. The far-field value of the material damping factor in all of these solutions is taken as $\tan \delta_o = 0.05$. The corresponding factors for the boundary of the hole are defined by equation(25).

In the light of the inaccuracies revealed by the comparison of the results presented in figure 5-2, the low-frequency behavior of the curves in figure 5-3, particularly those corresponding to the higher values of G_o/G_i, must be considered as suspect. There is no question, however, regarding the accuracy of the presented curves in the moderate and high frequency ranges. The curves for β_w in the latter figure have the same high-frequency limit, whereas those for α_w have different limits.

In the study of vertically excited layers presented in reference 8, it was noted that the high-frequency limit of α_w for a layer with no material damping and a continuous variation of shear modulus is given by

$$\alpha_w|_{a_i \to \infty} = 1 + \frac{1}{2} f'(1) \tag{36a}$$

in which $f'(1)$ = the slope of $G(\xi)$ at $\xi = 1$ normalized with respect to G_i. For the variation defined by equation (24), equation (36a) reduces to

$$\alpha_w|_{a_i \to \infty} = 1 + \frac{n}{2}\left(\frac{G_o}{G_i} - 1\right) \tag{36b}$$

As a demonstration of the reliability of equations (36) and as a further confirmation of the high-frequency behavior of the curves for β_w, the impedance coefficients for the bounded variation of shear modulus defined by equation (24) are compared in figure 5-4 with those obtained for the variation defined by equation (1a) without imposing an upper limit on ξ. Increasing without bound, the latter variation has been examined previously in reference 8 and by Gazetas and Dobry [1]. The exponents m and n in

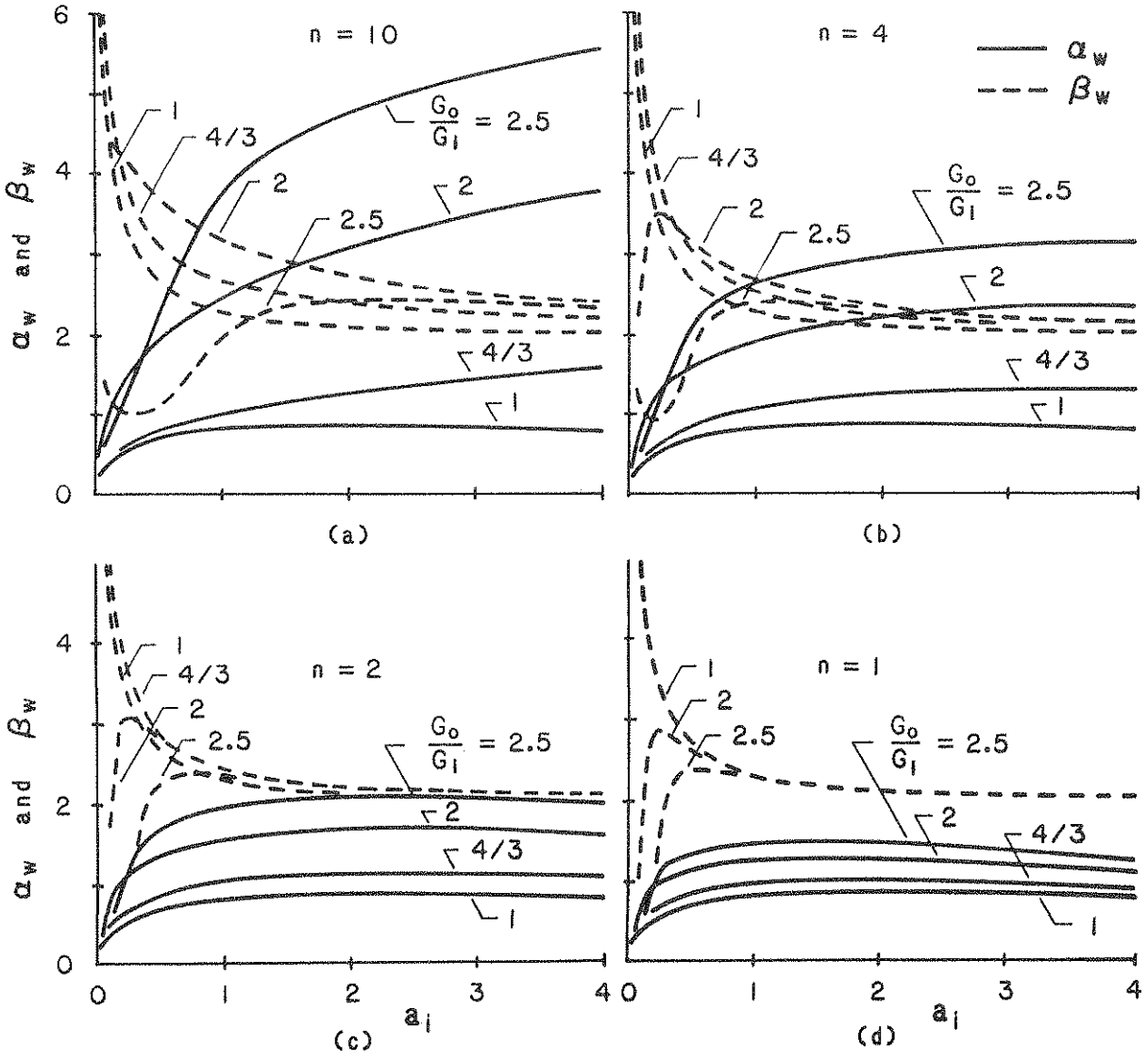

Figure 5-3. Impedance Coefficients for Vertically Excited Layers with Radial Variations of Shear Modulus Defined by Equation (23); $\tan \delta_o = 0.05$

the two expressions are chosen such the values of both the shear modulus and of its slope at the boundary of the hole are identical in the two cases. These conditions require that

$$m = n\left(\frac{G_o}{G_i} - 1\right) \tag{37}$$

The particular data displayed are for layers without material damping and a value of $G_o/G_i = 2$ for the bounded variation. Equation (37) in this case reduces to $m = n$.

Note that the high-frequency limits of both the stiffness and damping coefficients in figure 5-4 are identical for the two variations. Note further that there are significant differences between the two sets of data in the practically important range of a_i values of one or less. It follows that, within this frequency range, the unbounded variation should be used as a substitute for the more realistic bounded variations only with the greatest possible care. The errors in such usage would be expected to be particularly large for the higher values of m and n which are associated with rather abrupt modulus variations.

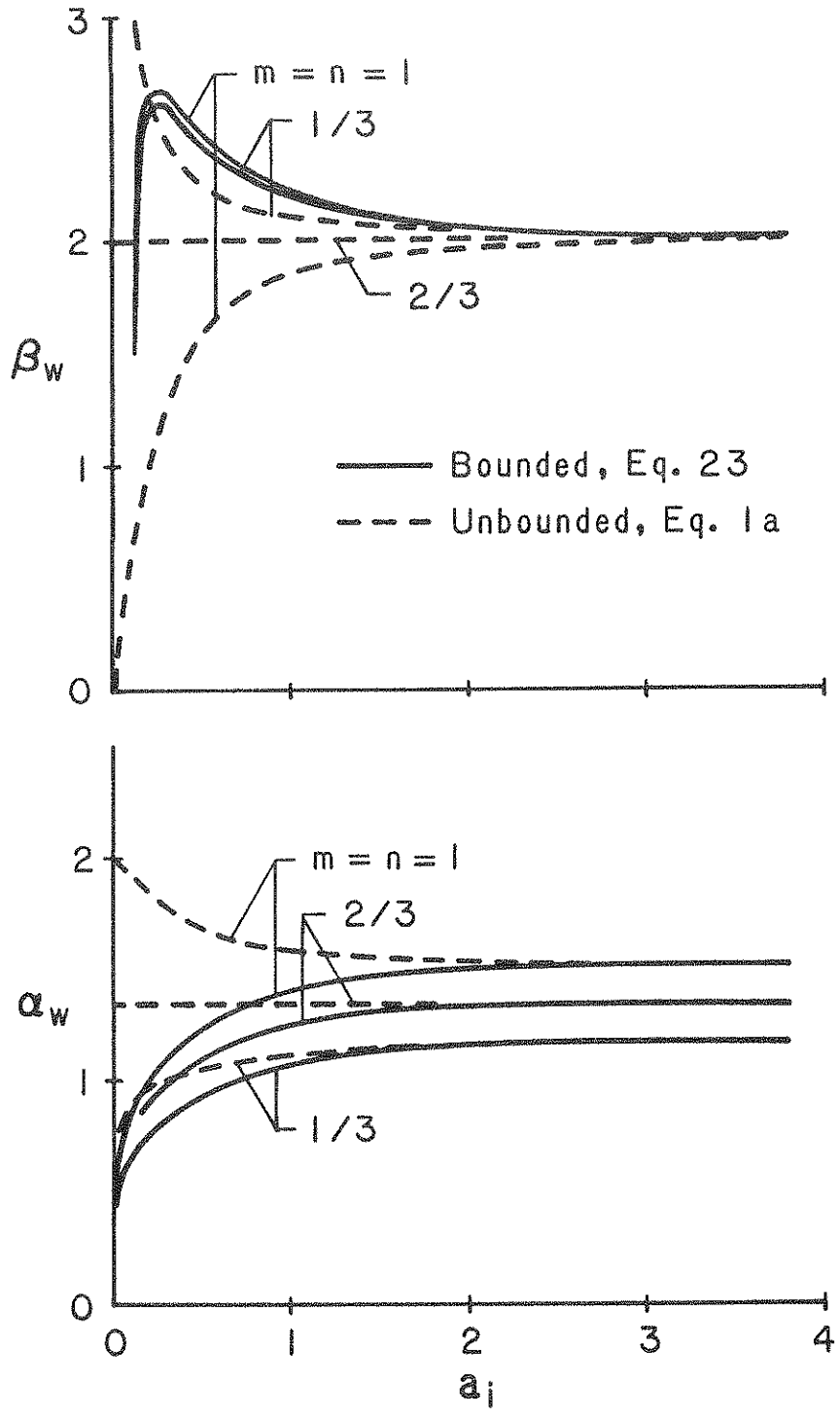

Figure 5-4. Comparisons of Impedance Coefficients for Vertically Excited Layers with Unbounded and Bounded Radial Variations of Shear Modulus; $\tan\delta = 0$; $f'(1) = m = n$

SECTION 6
CONCLUSION

With the information and insight into the response that have been provided in this paper, the vertical and torsional impedances of radially inhomogeneous viscoelastic soil layers with a circular hole and ramp-like, continuous variations in shear modulus may be evaluated readily. When plotted as a function of the frequency parameter, these impedances are not nearly as undulatory as those obtained for layers with discontinuous variations in material properties, but are not entirely without undulations due to the discontinuity in the slope of the shear modulus at the interface of the two zones. The high-frequency limit of the real part of the impedance function has been shown to be controlled by the values of the shear modulus and its slope at the boundary of the central hole.

SECTION 7

APPENDIX. SOLUTIONS OF EQUATIONS (5) AND (13) FOR m = 2

When the exponent in equation (1a) is m = 2, the differential equations governing the motion of the vertically excited layer reduce to

$$\xi^2 \frac{d^2w}{d\xi^2} + 3\xi \frac{dw}{d\xi} - \lambda_i^2 w = 0 \qquad \text{for } 1 \leq \xi \leq \xi_o \qquad (38a)$$

$$\xi^2 \frac{d^2w}{d\xi^2} + \xi \frac{dw}{d\xi} - \lambda_o^2 \xi^2 w = 0 \qquad \text{for } \xi \geq \xi_o \qquad (38b)$$

and those governing the torsionally excited layer reduce to

$$\xi^2 \frac{d^2v}{d\xi^2} + 3\xi \frac{dv}{d\xi} - (\lambda_i^2 + 3) v = 0 \qquad \text{for } 1 \leq \xi \leq \xi_o \qquad (39a)$$

$$\xi^2 \frac{d^2v}{d\xi^2} + \xi \frac{dv}{d\xi} - (\lambda_o^2 \xi^2 + 1) v = 0 \qquad \text{for } \xi \geq \xi_o \qquad (39b)$$

The solutions of equations (38) are

$$w = A_w \xi^{q_1} + B_w \xi^{q_2} \qquad \text{for } 1 \leq \xi \leq \xi_o \qquad (40a)$$

$$w = C_w K_o(\lambda_o \xi) + D_w I_o(\lambda_o \xi) \qquad \text{for } \xi \geq \xi_o \qquad (40b)$$

and those of equations (39) are

$$v = A_\theta \xi^{q_3} + B_\theta \xi^{q_4} \qquad \text{for } 1 \leq \xi \leq \xi_o \qquad (41a)$$

$$v = C_\theta K_1(\lambda_o \xi) + D_\theta I_1(\lambda_o \xi) \qquad \text{for } \xi \geq \xi_o \qquad (41b)$$

in which

$$q_1 = -1 + \sqrt{1 + \lambda_i^2} \qquad (42a)$$

$$q_2 = -1 - \sqrt{1 + \lambda_i^2} \qquad (42b)$$

$$q_3 = -1 + \sqrt{4 + \lambda_i^2} \tag{42c}$$

$$q_4 = -1 - \sqrt{4 + \lambda_i^2} \tag{42d}$$

$D_w = D_\theta = 0$; and A_w through C_θ are constants of integration which may be determined from the solution of the following systems of equations. Obtained by satisfying the appropriate boundary and interface conditions identified previously, the equations for the vertically excited layer are

$$\begin{bmatrix} 1 & 1 & 0 \\ \xi_o^{q_1} & \xi_o^{q_2} & -K_0(\lambda_o\xi_o) \\ q_1\xi_o^{q_1} & q_2\xi_o^{q_2} & \dfrac{1 + i\tan\delta_o}{1 + i\tan\delta_i}(\lambda_o\xi_o)K_1(\lambda_o\xi_o) \end{bmatrix} \begin{Bmatrix} A_w \\ B_w \\ C_w \end{Bmatrix} = \begin{Bmatrix} 1 \\ 0 \\ 0 \end{Bmatrix} \tag{43}$$

and those for the torsionally excited layer are

$$\begin{bmatrix} 1 & 1 & 0 \\ \xi_o^{q_3} & \xi_o^{q_4} & -K_1(\lambda_o\xi_o) \\ (q_3 - 1)\xi_o^{q_3} & (q_4 - 1)\xi_o^{q_4} & \dfrac{1 + i\tan\delta_o}{1 + i\tan\delta_i}(\lambda_o\xi_o)K_2(\lambda_o\xi_o) \end{bmatrix} \begin{Bmatrix} A_\theta \\ B_\theta \\ C_\theta \end{Bmatrix} = \begin{Bmatrix} R \\ 0 \\ 0 \end{Bmatrix} \tag{44}$$

With the integration constants determined, the impedances of the vertically excited layer are computed from equation (12a) to be

$$K_w = -2\pi G_i^* (A_w q_1 + B_w q_2) \tag{45}$$

and those of the torsionally excited layer are computed from equation (16a) to be

$$K_\theta = -2\pi G_i^* R [A_\theta(q_3 - 1) + B_\theta(q_4 - 1)] \tag{46}$$

SECTION 8
NOTATION

a_i	dimensionless frequency parameter for inhomogeneous layer, defined by equation (7)
a_o	dimensionless frequency parameter for homogeneous layer, defined by equation (9)
A_w, B_w	
C_w, D_w	constants of integration for vertically excited layer
A_θ, B_θ	
C_θ, D_θ	constants of integration for torsionally excited layer
C_o to C_7	coefficients in polynomial defined by equation (32)
$f'(1)$	value of $G'(\xi)$ at $\xi = 1$ normalized with respect to G_i
$g(\xi)$	$G^*(\xi)$ normalized with respect to G_i
$G(\xi)$	shear modulus of elasticity for material of layer at ξ
G_i	shear modulus of elasticity for material at the boundary of the hole
G_o	shear modulus of elasticity for material in undisturbed outer zone
$G^*(\xi)$	complex-valued shear modulus of elasticity for material of layer at ξ
G_i^*	value of $G^*(\xi)$ for material at the boundary of the hole
G_o^*	value of $G^*(\xi)$ for material in undisturbed outer zone
i	$\sqrt{-1}$
I_κ	modified Bessel function of first kind of order κ
K_κ	modified Bessel function of second kind of order κ
K_w	vertical dynamic impedance of soil layer
K_θ	torsional dynamic impedance of soil layer

m	constant in equation (1) that defines variation of $G^*(\xi)$
n	constant in equation (24) that defines variation of $G^*(\xi)$
q_1, q_2, q_3, q_4	complex-valued dimensionless parameters defined by equation (42)
r	radial distance to arbitrary point
R	radius of central circular hole
R_o	radius of interface of inner and outer zones of soil layer
t	time
$\tan \delta_i$	damping factor for material at the boundary of the hole
$\tan \delta_o$	damping factor for material of undisturbed outer zone
v	circumferential displacement for arbitrary point on layer
v_{si}	shear wave velocity for material at the boundary of the hole
v_{so}	shear wave velocity for material in undisturbed outer zone
w	vertical displacement for arbitrary point on layer
α_w	stiffness coefficient for vertically excited layer
α_θ	stiffness coefficient for torsionally excited layer
β_w	damping coefficient for vertically excited layer
β_θ	damping coefficient for torsionally excited layer
γ	constant in equation (29) for vertical displacement
ΔR	width of softened boundary zone
κ	$2/(2-m)$
λ_i	dimensionless parameter defined by equation (6)
λ_o	dimensionless parameter defined by equation (8)
ξ	r/R = dimensionless radial position coordinate
ξ_o	R_o/R
ρ	mass density for material of layer
τ_{rz}	vertical shearing stress at arbitrary point on layer

ϕ approximating function for vertical displacement

χ $\sqrt{G_o^*/G_i^*}$

ω circular frequency of excitation and of resulting steady-state response

SECTION 9

REFERENCES

1. Gazetas, G., and Dobry, R., "Simple Radiation Damping Model for Piles and Footings," Journal of Engineering Mechanics, ASCE, Vol. 110, No. 6, June 1984, pp. 937-956.

2. Lakshmanan, N., and Minai, R., "Dynamic Soil Reactions in Radially Non-Homogeneous Soil Media," Bulletin of the Disaster Prevention Research Institute, Kyoto University, Vol. 31, Part 2, No. 279, June 1981, pp. 79-114.

3. Novak, M., "Dynamic Stiffness and Damping of Piles," Canadian Geotechnical Journal, Vol. 11, No. 4, 1974, pp. 574-598.

4. Novak, M., Nogami, T., and Aboul-Ella, F., "Dynamic Soil Reactions for Plane Strain Case," Research Report, BLWT-1-77, Faculty of Engineering Science, The University of Western Ontario, London, Ontario, Canada, June 1977, pp. 1-26.

5. Novak, M., Nogami, T., and Aboul-Ella, F., "Dynamic Soil Reactions for Plane Strain Case," Journal of the Engineering Mechanics Division, ASCE, Vol. 104, No. EM4, August 1978, pp. 953-959.

6. Novak, M., and Sheta, M., "Approximate Approach to Contact Effects of Piles," Special Technical Publication on Dynamic Response of Pile Foundations: Analytical Aspects, ASCE, M. W. O'Neill and R. Dobry, eds., October 1980, pp. 53-79.

7. Veletsos, A. S., and Dotson, K. W., "Impedances of Soil Layer with Disturbed Boundary Zone," Journal of Geotechnical Engineering, ASCE, Vol. 112, No. 3, March 1986, pp. 363-368.

8. Veletsos, A. S., and Dotson, K. W., "Vertical and Torsional Vibration of Foundations in Inhomogeneous Media," Technical Report NCEER-87-0010, National Center for Earthquake Engineering Research, State University of New York at Buffalo, June 1987.

9. Veletsos, A. S., and Dotson, K. W., "Horizontal Impedances for Radially Inhomogeneous Viscoelastic Soil Layers," Technical Report NCEER-87-0021, National Center for Earthquake Engineering Research, State University of New York at Buffalo, October 1987.

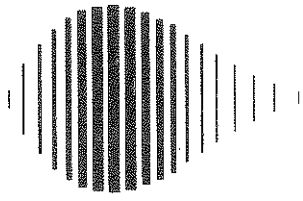

National Center for Earthquake Engineering Research
State University of New York at Buffalo